



Evaluation of peripheral effects during leg penetration and withdrawal by centrifuge loading model tests in alternating soil layers and reproduction analysis by MPM analysis

Y. Maeda*, K. Suzuki

Offshore Wind Energy Dept., Shimizu Corporation, Tokyo, Japan

T. Kiriyaama, H. Sugiyama

Institute of Technology, Shimizu Corporation, Tokyo, Japan

**maeda.y@shimz.co.jp (corresponding author)*

ABSTRACT: Numerous offshore wind power projects are currently under development in Japan. Certain regions in Japan are characterized by the presence of thick alluvial clay deposits within the intermediate strata, necessitating careful consideration of the surrounding effects caused by deep leg penetration. In this study, centrifuge loading model tests are employed to assess the impact of leg penetration on the port infrastructure and bearing capacity in alternating soil layers. The experimental results elucidate the characteristics of the surrounding effects and the bearing capacity of alternating soil layers. Moreover, these phenomena are successfully reproduced using the material point method (MPM) analysis, indicating the potential for further advancements in this analytical approach.

Keywords: Leg penetration; centrifuge loading model tests; MPM analysis; surrounding effects

1 INTRODUCTION

Numerous offshore wind power projects are planned as part of the Green Growth Strategy in Japan (Ministry of Economy, Trade, and Industry 2020). To achieve its 2030 target, the Japanese government is developing base ports to support these projects. During the execution phases of these projects, self-elevating platform (SEP) vessels are deployed adjacent to the wharves to facilitate the lifting of various components. Excessive leg penetration beyond anticipated levels may pose potential risks to the structural integrity of the wharf.

Furthermore, certain regions in Japan are characterized by thick alluvial clay deposits within the intermediate strata and require deeper leg penetration to ensure adequate soil-bearing capacity. Consequently, it is imperative to consider the adverse effects on the surrounding environment.

Studies involving leg penetration have been conducted (Kencana 2021; Tanaka et al. 2024). However, previous investigations on the peripheral effects of leg penetration in alternating soil layers remain limited, and comprehensive knowledge has not been developed.

This study employs centrifuge loading model tests and material point method (MPM, Sulsky et al. 1994) analyses to assess the impact of leg penetration on port facilities in alternating soil layers.

2 LEG PENETRATION AND WITHDRAWAL INTO ALTERNATING SOIL LAYERS

To simulate the peripheral effects during leg penetration and withdrawal in alternating soil layers, a spudcan model was developed and centrifuge loading model tests were performed. To minimize scale effects, a centrifuge at the National Research and Development Agency Public Works Research Institute ([PWRI](#)), one of the largest centrifuges in Japan, was used in the experiment.

2.1 Experimental outline

The centrifuge employed in the experiment had a radius of 6.6 m and a loading capacity of 400 t G. The centrifugal acceleration (G) was set to 75 G. The soil tank was a rigid aluminium container measuring 1.5 m (112.5 m in prototype scale) in width, 0.5 m (37.5 m) in height, and 0.5 m (37.5 m) in depth, with Teflon

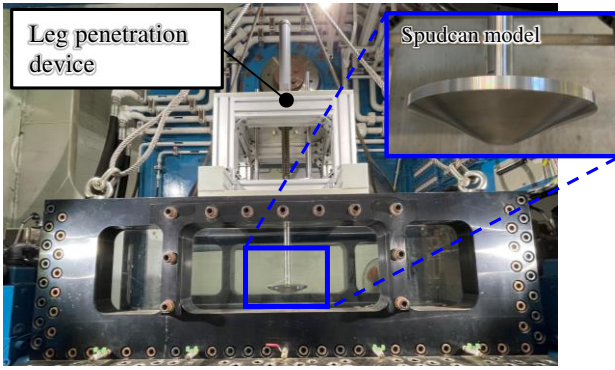


Figure 1. Leg penetration device and spudcan model.

sheets lining the inner surfaces to reduce friction between the soil and the tank.

The spudcan model (diameter $D = 191$ mm; 14.3 m in the prototype), representing the tip of the leg penetrating the ground, was designed by simplifying the shape of the SEP vessel “BLUE WIND” owned by the Shimizu Corporation to a conical form with an equivalent flat area. The leg penetration device, shown in Figure 1, was electrically controlled with a loading stroke of 500 mm (37.5 m) and a load capacity of 50 kN (281 MN). A load cell was incorporated in the leg to measure the applied load.

To assess the peripheral effects of the lateral pressure induced by leg penetration, observation piles (aluminum) were placed every $0.5 D$ from the edge of the spudcan at a distance of 0.5 to $3 D$. Strain gauges were attached to the observation piles at heights of 1–7 m, as shown in Figure 2. The soil deposits were composed of Ds, Ac, and As (silica no. 7 for the sand and kaolin for the clay layer). The Ds layer was compacted by tamping to a relative density (Dr) of 95%, and the Ac layer was created by consolidating it using centrifugal force. After consolidation of the Ac layer was completed, the As layer was compacted to a Dr value of 70%.

The spudcan model penetrated at a rate of 10 mm/min and stopped upon reaching a predetermined load level (designated as the preload load), after which the leg was withdrawn. The deformation of the ground after withdrawal was observed by examining the cross-section of the soil tank. Two cases were considered using the soil thickness conditions shown in Figure 2.

2.2 Experimental results

2.2.1 Leg penetration depth

Figure 3 shows the cross-section of the soil tank after penetration in Case 1. Markers installed beforehand to assess the deformation showed that lateral extrusion occurred at the bottom end of the Ac layer, whereas retraction occurred at the surface layer.

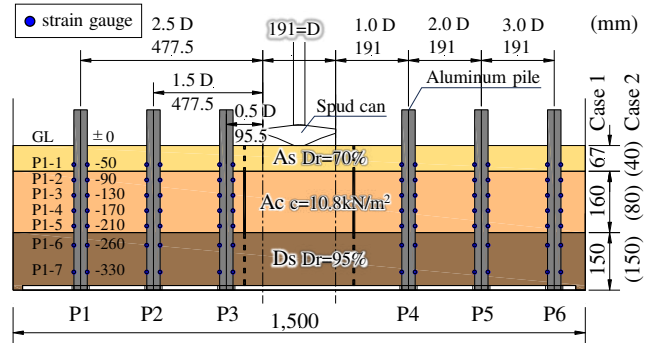


Figure 2. Schematic of leg penetration peripheral effects measurement in soil tanks.

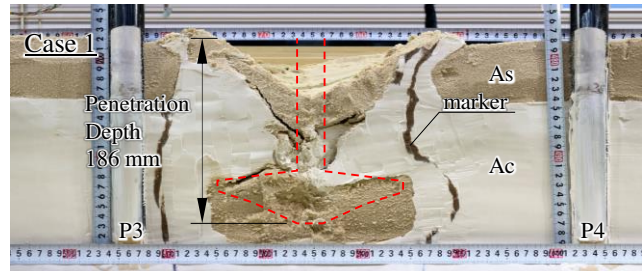


Figure 3. Soil tank cross-sectional conditions after leg penetration and extraction.

Figure 4(a) shows the time history of the spudcan tip depth. The penetration ceased when the bearing capacity reached its maximum value (M), which was equal to the preload load. The penetration depths were 186 and 105 mm in Cases 1 and 2, respectively. Both depths were the heights before reaching the Ds layer. The sand plug thickness was 60–80% of the thickness of the As layer.

2.2.2 Measurement of peripheral effects

Figures 4(b) and (c) show the time histories of the bending moments along the observation pile (P4) for

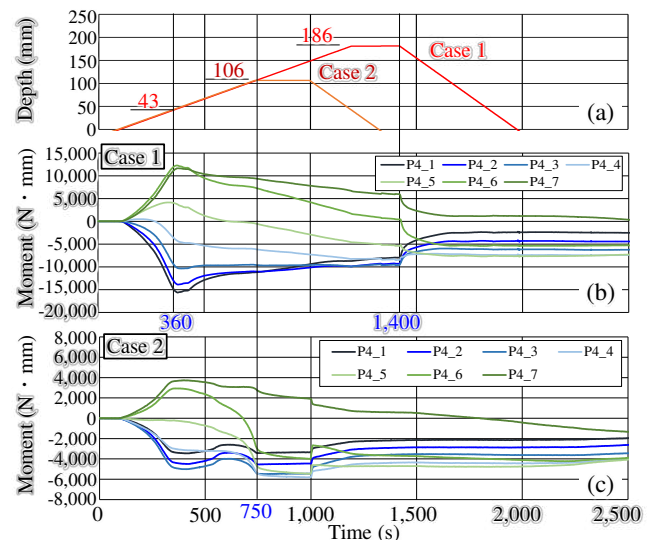


Figure 4. (a) Spudcan depth and (b and c) bending moments on the observation pile.

Cases 1 and 2, respectively. In Case 1, the bending moment reached its M at approximately 360 s (GL = -43 mm) during the penetration of the As layer (GL = 0 to -67 mm). It then decreased during the penetration of the Ac layer and decreased further after withdrawal began at 1400 s (GL = -186 mm). In Case 2, the bending moment decreased after penetration of the As layer (GL = 0 to -40 mm), as in Case 1, but reached M at the maximum penetration depth (GL = -106 mm). The difference in the timing of the maximum occurrence of the peripheral effect was due to the thickness of the clayey soil. In Case 1, where the clayey soil was thick, the pull-in during clayey soil penetration was large. Therefore, M was assumed to have occurred when the surface sand layer was penetrated. Even after withdrawal, a residual bending moment of approximately 20–30% of the peaks remained.

2.2.3 Correlation between separation and lateral ground pressure

Figure 5 shows the sectional forces generated in each observation pile (P1–P6) in Case 1. Particularly at P3 and P4 near the spudcan, the sectional forces reached their peaks during sand layer penetration and then uniformly decreased, with a residual value remaining even after withdrawal.

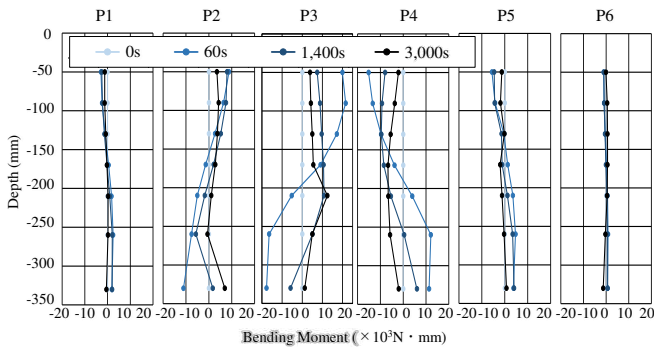


Figure 5. Bending moments on the observation pile in Case 1.

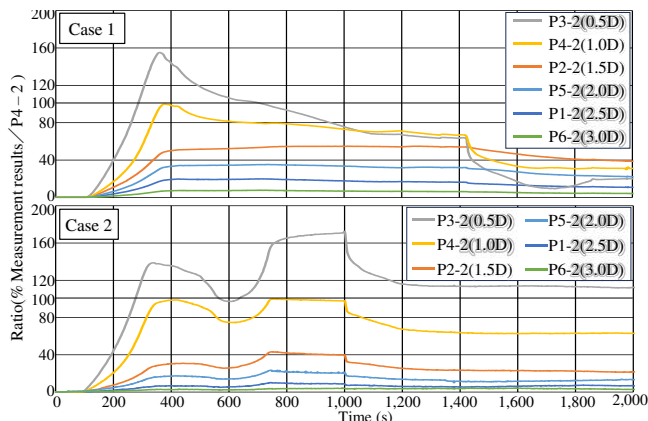


Figure 6. Correlation between separation and bending moment.

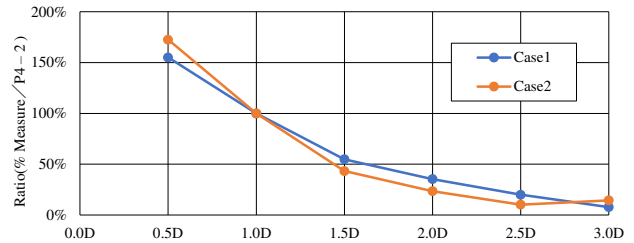


Figure 7. Correlation between separation and bending moment.

Comparing Cases 1 and 2 in Figure 4, the generated cross-sectional force was reduced to less than 40% owing to a 56% reduction in penetration. From this perspective, the peripheral effect was assumed to be correlated with penetration. The maximum cross-sectional forces occurred at different times: at the time of sand and maximum penetration in Cases 1 and 2, respectively.

Figure 6 shows the time histories of the bending moments normalized by M , with P4 at 1.0 D from the spudcan edge used as the reference. Figure 7 shows that the reduction in peripheral effects by separation was not significantly different in each case: approximately 50, 30, 20, and 10% at 1.5, 2.0, 2.5, and 3.0 D, respectively, based on 1.0 D at P4.

These comparisons showed that M of the peripheral effect in the alternating soil layers correlated with the amount of penetration; however, the decrease in the effect with separation did not differ significantly with penetration. To verify this correlation, verification with layer thickness and strength as parameters is required. Therefore, the following section presents an analytical approach.

3 REPRODUCTION OF THE EXPERIMENT USING THE MATERIAL POINT METHOD

To analytically predict the spudcan penetration resistance in ground with a stratum structure different from that used in the experiment, an analytical model was constructed to reproduce the experiment.

3.1 Numerical method for spudcan penetration

Spudcan penetration into the ground support involves a large deformation. Spudcan penetration simulations were numerically performed using mesh- and particle-based methods. The coupled Eulerian-Lagrangian (CEL) analysis technique was employed for spudcan penetration to demonstrate the validity of the method and the numerical conditions required to reproduce the experimental results and its effect on adjacent piles (Tho et al. 2012; 2013; Fan and Wang 2021). The CEL approach has also been applied to three-dimensional

problems to understand the spudcan shape effect (Fan et al. 2021). The large-deformation finite element (FE) approach was also applied to assess partially drained ground conditions (Liu et al. 2022). More recently, the MPM has been applied for spudcan penetration (Li 2023). Brinkgreve et al. (2015) and Pradhan et al. (2023) applied the MPM to simulate spudcan penetration in interlayered ground, thereby verifying the applicability of this method.

3.1.1 Particle–element coupled method

When conventional mesh-based FE analysis is applied to the spudcan penetration simulation, mesh-tangling occurs, and the method is not able to continue the simulation. Alternatively, when the remeshing technique is employed, remeshing induces an intensive increase in the numerical cost. To overcome these numerical difficulties, a particle-based method was employed in this study.

An analysis code based on the MPM was developed. The computational efficiency of the developed code was enhanced for practical use by combining particle and element models, using the particle-element coupled method (PEM) (Kiriya and Higo 2020). In the MPM framework, the physical quantities are carried by the material point (MP), whereas the equation of motion is solved at the numerical grid point. A characteristic of the PEM is that the domain subjected to a small deformation is modelled by elements, whereas the domain subjected to a large deformation is modelled by particles. As the domain subjected to large deformations is relatively limited in the entire domain, the combination of the element and particle approaches realizes intensive computational efficiency.

3.1.2 Constitutive model for spudcan penetration

An elastic-plastic constitutive model with both the yield and potential functions of the Mohr–Coulomb criterion with strain softening was employed for the geomaterial. The material properties of the soil strata were determined by laboratory elemental tests. The soil specimens for laboratory tests were sampled from the soil tank after the experiment. The spudcan was modelled by elastic material.

3.2 Numerical model and conditions

In this study, a PEM with an axisymmetric formulation (Kiriya and Higo 2022) was used to model 3D phenomena with half planar model geometry. The computational domain in the prototype was divided into two regions: the region near the spudcan was modelled with particles using MPM, and the region

Table 1. Analytical soil properties.

Layer	ϕ (°)	C (kN/m ²)	E (kN/m ²)	γ' (kN/m ²)	ν
As	40.8	5.6	7,500	4.7	0.33
Ac	8.3	10.8	1,500	5.9	0.45
Ds	40.6	25.1	20,000	5.8	0.33

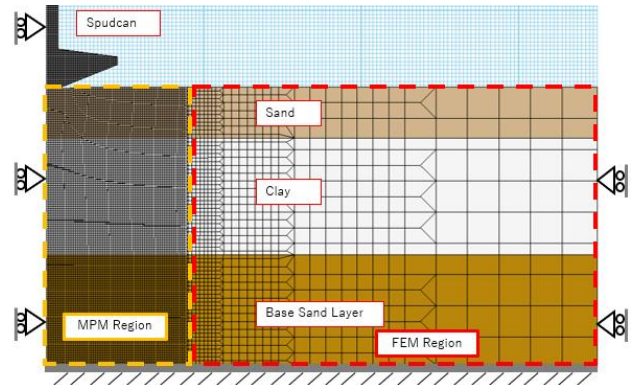


Figure 8. Analytical model.

distant from the spudcan was modelled with elements to reduce the computational cost required for the simulation (Figure 8). In Figure 8, the left side shows the axisymmetric center. Both the left and right sides were subjected to the vertical roller condition (horizontally fixed), and the bottom boundary was fixed horizontally and vertically. The external force was applied to the spudcan model by increasing the body force of the spudcan incrementally, whereas the actual external force in the experiment was controlled by the displacement.

3.3 Analysis of Results

3.3.1 Process of spudcan penetration

Figure 9(a) shows the soil layer distribution explaining the soil plug formation under the spudcan end-tips obtained from the analysis. The formation of the sand plug is explained as follows: the surface sand layer was pushed downward, forming a dent (Figure 9(a)-(i)); the dent was pushed down farther (Figure 9(a)-(ii)); the dent was separated from the surface sand layer (Figure 9(a)-(iii)); and the sand plug was formed (Figure 9(a)-(iv)). In the experiment, only the final shape was observed after centrifugal loading, while the PEM enabled visualization of the process of sand plug formation. Figure 9(b) shows the displacement contour during spudcan penetration, indicating that the surface sand layer (As) under the spudcan was mainly deformed in the vertical direction, whereas the intermediate clay layer (Ac) was deformed in both the vertical and horizontal directions. The laterally deformed area was within 1 D of the spudcan diameter from its side end.

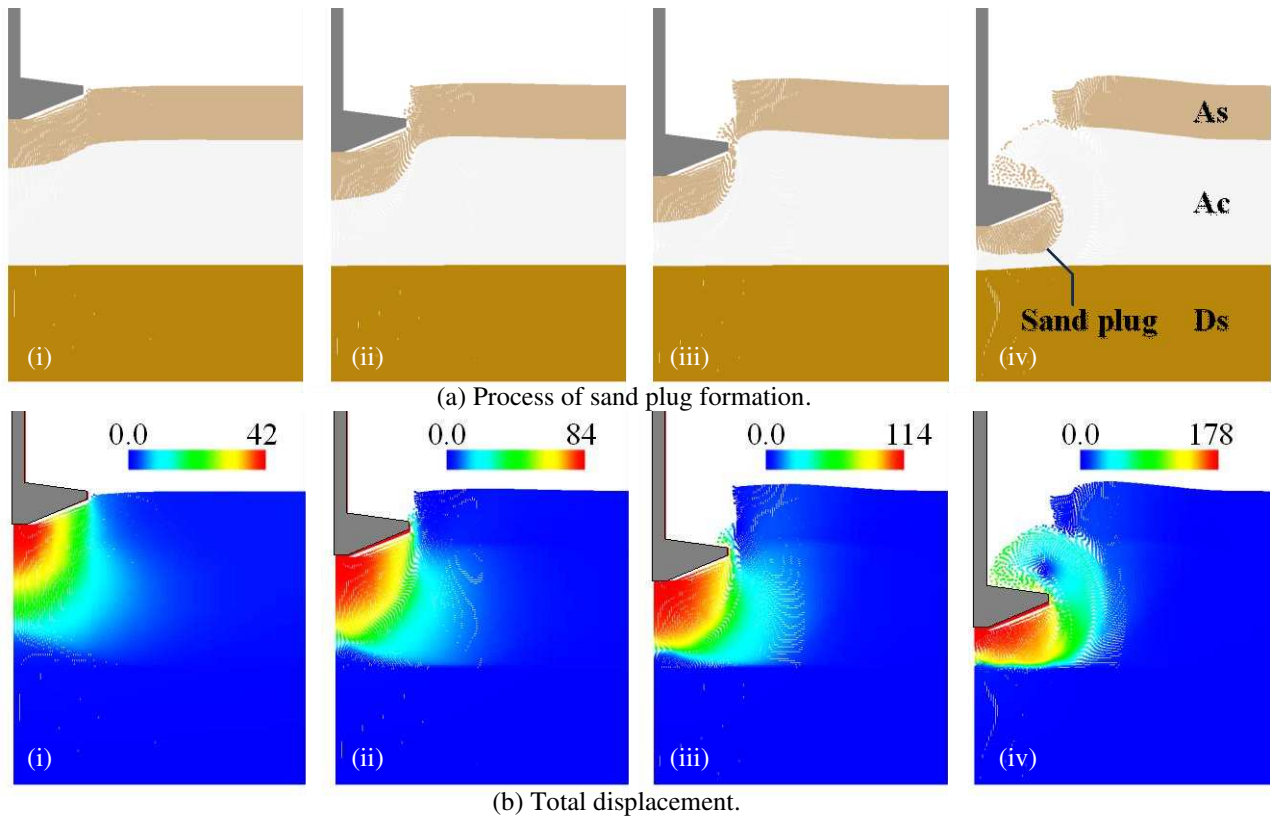


Figure 9. Soil layer distribution and total displacement contours.
(i) Depth = 42 mm, (ii) 84 mm, (iii) 114 mm, and (iv) 178 mm.

The experimental results for the sand plugs, lateral extrusion of the lower Ac layer, and retraction of the upper Ac layer in the leg direction are qualitatively shown in Figure 3. Additionally, the penetration depth was 178 mm (13.6m in the prototype), which was approximately 98% of the experimental value of 186 mm (13.9 m), indicating that the behavior of each soil layer owing to leg penetration was accurately reproduced in the simulation.

3.3.2 Penetration resistance and tip depth

Figure 10 shows the relationship between penetration resistance and spudcan tip depth. The reference numbers from (i) to (iv) in Figure 10 correspond to those in Figure 9. The penetration resistance in the experiment increased as the tip depth in the As layer increased to approximately 50 mm, and then began to decrease or remained constant, showing a steep increase in the tip depth. This was because the overburden pressure on the Ac layer exceeded the bearing capacity, exhibiting punch through penetration. The penetration resistance increased again after punch through as its tip became close to the Ds layer because of its high strength. As shown in Figure 9, because the spudcan dragged the As layer as a sand plug under its tip, the penetration resistance recovered before reaching the Ds layer.

The simulation results in Figure 10 show almost the same curves as the experimental results up to the first peak in the As layer. The punch through penetration is expressed as a gradual increase in resistance. One reason for the difference between the experimental and simulation results during punch through is the external force control: displacement in the experiment and force in the simulation. However, the final tip depth and penetration resistance obtained from the simulation were almost identical to those obtained experimentally.

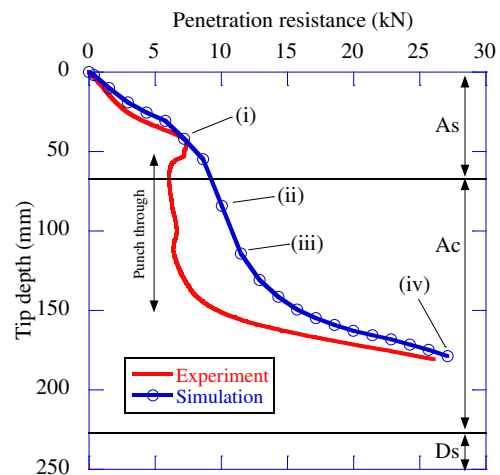


Figure 10. Relationship between ground resistance and penetration (model scale).

4 CONCLUSION

The centrifugal-load model experiment and MPM analysis provided the following insights:

- Under ground conditions where a sand layer (As) exists on the surface and a thick layer of soft clay (Ac) is deposited in the middle layer, the peripheral effect caused by leg penetration reaches its M during the penetration of the surface layer. This tendency is particularly pronounced with small separation from the spudcan.
- If the bending moment measured at a separation of 1.0 D (P4) is considered as the reference point at 100%, then the M that occurs in each pile is approximately 50, 30, 20, and 10% at 1.5, 2.0, 2.5, and 3.0 D, respectively. Attenuation of the impact with distance was confirmed.
- The MPM analysis successfully reproduced most of the experimental behaviors, including soil deformation, sand plugs, and leg penetration.

However, in this experiment, the measurement piles were arranged in a straight line, which may have reduced the impact due to the presence of piles in the front. In an actual project with ground conditions similar to those assumed in this study, measurement data from a multistage inclinometer during leg penetration at the front of the quay wall and its effects on the quay wall structure were accumulated during jack-up with a root penetration of 1.0 D or greater. Based on the results of this study, further research should examine methods for assessing the peripheral effects of leg penetration using accumulated data.

AUTHOR CONTRIBUTION STATEMENT

First Author: Conducting the experiments, data management, formal analysis, and writing the original draft. **Additional authors:** MPM analysis, software utilization, conception, supervision, writing, review, and editing.

ACKNOWLEDGEMENTS

The authors thank the PWRI and NOM Co., Ltd. for their technical assistance with the centrifuge tests. The project described in this paper was conducted based on the our development budget.

REFERENCES

Brinkgreve, R. B. J. et al. (2015). Beyond the Finite Element Method in Geotechnical Analysis. *BAW Mitteilungen* Nr. 98 2015. Delft University of Technology & Plaxis BV.

- Fan, L., Gao, P., Wang, F., and Duan, M. (2021). Experimental and Numerical Investigation on Cavity Formation from Large Rectangular Spudcan Penetration in clay, *Applied Ocean Research*, 108.
- Fan, Y., and Wang, J. (2021). Method o Evaluate Effect of Spudcan Penetration on Adjacent Jacke Piles, *Applied Ocean Research*, 106.
- Kencana, E. Y. (2021). *Numerical study of spudcan-pile interaction*. Dissertation submitted for the degree of Doctor of Philosophy, National University of Singapore, Singapore. Available at: <https://scholarbank.nus.edu.sg/handle/10635/190517>, accessed: 30/08/2024.
- Kiriyaama, T., and Higo. Y. (2020). Arbitrary particle domain interpolation method and application to problems of geomaterial deformation, *Soils and Foundations*, 60(6), 1422-1439.
- Kiriyaama, T., and Higo. Y. (2022). Axisymmetric Particle-Element Coupled Method for Deformation Problems of Geomaterial, *Soils and Foundations*, 62(5), 101180-1-12.
- Li, Y. (2023). Simulation of Rapid Spudcan Penetration with the Material Point Method. Dissertation submitted for the degree of Doctor of Philosophy, University of Western Australia.
- Liu, K., Wang, D., and Zheng, J. (2022). Numerical investigation of spudcan penetration under partilly drained conditions, *Ocean Engineering*, 244.
- Ministry of Economy, Trade and Industry (2020). Green Growth Strategy For Carbon Neutrality by 2050. Available at: [\[https://www.meti.go.jp/policy/energy_environment/global_warming/ggs/index.html\]](https://www.meti.go.jp/policy/energy_environment/global_warming/ggs/index.html), accessed: 30/09/2024.
- Pradhan, M. et al. (2023). Applicability of Particle Method for Analyzing Peripheral Effect During SEP Vessel Leg Penetration. In: *Reiwa 5th National Conference of the Japan Society of Civil Engineers*, Hiroshima, Japan. Public Work Research Institute, B-Block B9 Large-scale Geotechnical Dynamic Centrifuge. Available at: [\[https://www.pwri.go.jp/eng/about/facility/facility/b_b9.html\]](https://www.pwri.go.jp/eng/about/facility/facility/b_b9.html), accessed: 30/09/2024.
- Sulsky, D., Chen, Z. and Schreyer, H.L. (1994). A Particle Method for History-dependent Materials. *Comput. Methods Appl. Mech. Engrg.* 118, 179–196.
- Tanaka, F. et al. (2024). Analysis of the Impact on the Quay and Dynamic Observation Results of Construction by SEP Vessel at Ishikari Bay New Port. In: *Reiwa 6th National Conference of the Japan Society of Civil Engineers*, Hokkaido, Japan.
- Tho, K.K., Leung, C.F., Chow, Y.K., and Swaddiwudhipong, S. (2012). Eulerian Finite-Element Technique for Analysis of Jack-Up Spudcan Penetration, *ASCE, International Journal of Geomechanics*, 12(1), 64-73.
- Tho, K.K., Leung, C.F., Chow, Y.K., and Swaddiwudhipong, S. (2013). Eulerian finite element simulation of spudcan-pile interaction, *Canadian Geotechnical Journal*, 50, 595-608.

INTERNATIONAL SOCIETY FOR SOIL MECHANICS AND GEOTECHNICAL ENGINEERING



This paper was downloaded from the Online Library of the International Society for Soil Mechanics and Geotechnical Engineering (ISSMGE). The library is available here:

<https://www.issmge.org/publications/online-library>

This is an open-access database that archives thousands of papers published under the Auspices of the ISSMGE and maintained by the Innovation and Development Committee of ISSMGE.

The paper was published in the proceedings of the 5th International Symposium on Frontiers in Offshore Geotechnics (ISFOG2025) and was edited by Christelle Abadie, Zheng Li, Matthieu Blanc and Luc Thorel. The conference was held from June 9th to June 13th 2025 in Nantes, France.